TUDelft

Delft University of Technology

Characterization of bainitic/martensitic structures formed in isothermal treatments below the M$_s$ temperature

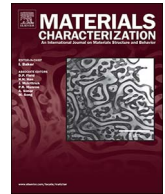Navarro-López, A.; Hidalgo Garcia, J.; Sietsma, J.; Santofimia Navarro, M.J.

Important note
To cite this publication, please use the final published version (if applicable).
Please check the document version above.

Characterization of bainitic/martensitic structures formed in isothermal treatments below the M$_s$ temperature

A. Navarro-López*, J. Hidalgo, J. Sietsma, M.J. Santofimia

Department of Materials Science and Engineering, Delft University of Technology, Mekelweg 2, 2628 CD Delft, The Netherlands

ABSTRACT

Advanced Multiphase High Strength Steels are generally obtained by applying isothermal treatments around the martensite start temperature (M_s). Previous investigations have shown that bainitic ferrite can form from austenite in isothermal treatments below M_s, where its formation kinetics is accelerated by the presence of the athermal martensite. That athermal martensite is tempered during the isothermal treatment, and fresh martensite may form during the final cooling to room temperature. The distinction between product phases present after the application of this type of heat treatments is difficult due to morphological similarities between these transformation products. The aim of this study is to characterize the structural and morphological features of the product phases obtained in isothermal treatments below the M_s-temperature in a low-carbon high-silicon steel. Multiphase microstructures, having controlled fractions of product phases, were developed by applying isothermal treatments above and below M_s, and were further studied by electron back scatter diffraction (EBSD) and scanning electron microscopy (SEM). The bainitic or martensitic nature of these product phases is discussed based on this characterization. Results showed that bainitic ferrite appears in the form of acicular units and irregularly shaped laths. Tempered martensite appears as laths with a sharp tip and as relatively large elongated laths with wavy boundaries containing protrusions.

1. Introduction

The development of new Advanced High Strength Steels (AHSS) requires the implementation of improved processing routes in which the resulting microstructures present a high degree of complexity. That is the case of multiphase steels obtained by applying isothermal holdings around the martensite start temperature (M_s) after austenitization, leading to microstructures generally formed by a mixture of martensite (fresh and/or tempered), bainite, and retained austenite. The presence of different product phases from austenite decomposition depends on whether the isothermal holding is applied at a temperature above M_s or below M_s.

After holding at a temperature above M_s and further quench, researchers agree that, in hypoeutectoid steels, the matrix is mainly formed by bainitic structures with retained austenite in the form of thin films and/or martensite-austenite (MA) islands [1–7]. Bainite is thus the isothermal product obtained from the decomposition of austenite. Carbides can also be present in bainite, depending on the composition of the steel and the isothermal holding temperature and time. Below M_s, however, the nature of the products formed during isothermal holding

is unclear due to the coexistence of product phases with morphological similarities such as tempered martensite and bainite.

Cooling from austenitization to a temperature between the martensite start (M_s) temperature and room temperature (RT) leads to the formation of a certain volume fraction of athermal martensite. This martensite has a strong accelerating effect on the subsequent transformation kinetics, mainly due to a higher density of potential nucleation sites [8–11]. Although bainite has been reported in hypoeutectoid steels as an isothermal decomposition product from austenite in isothermal treatments below M_s [4,10–14], there is experimental evidence showing the formation of other types of product phases in similar heat treatments. For example, several authors observed an isothermal product characterized by wide laths with characteristic wavy boundaries with ledges [16,17]. Kim et al. [7,15,16] stated that this isothermal product is neither purely martensitic nor purely bainitic, since it shows similarities with both types of product phases. Somani et al. [17] identified this product as isothermal martensite since it presents clear similarities to athermal martensite. According to the literature, isothermal martensite has mainly been reported in high-carbon steels and high-nickel alloys [18–20], but not in hypoeutectoid

steels. Independently of the growth mechanism of these product phases, the dilemma is which microstructural features observed in isothermal treatments below M_s correspond to each phase formed in those treatments, such as bainitic ferrite, tempered martensite or fresh martensite.

The goals of this study are: to characterize the microstructural features obtained in isothermal treatments performed at temperatures above and below M_s; relate those features to the product phases formed at each isothermal temperature; and determine, based on that characterization, the martensitic or bainitic nature of those product phases. For this purpose, isothermal heat treatments were applied at different temperatures around the M_s-temperature that were selected based on a previous study [11]. Various microstructures formed by combinations of different volume fractions of bainitic ferrite, tempered martensite, and fresh martensite were created. Volume fractions of those product phases were extracted from the dilatometry results presented in earlier work [11]. The identification of phases by dilatometry in combination with the characterization of microstructures formed at different temperatures by electron backscatter diffraction (EBSD) and scanning electron microscopy (SEM) provided a straight and systematic way of phase analysis.

2. Experimental procedure

The chemical composition of the investigated steel is 0.2C-3.51Mn-1.52Si-0.25Mo-0.04Al (wt. pct). The as-received material was hot rolled into a 4 mm-thick steel slab. Dilatometry specimens were extracted from hot rolled slabs, parallel to the rolling direction. These were cylindrical of dimensions 10 mm in length and 3.5 mm in diameter. Heat treatments were carried out in a Bähr 805A dilatometer. Specimens were placed between two quartz rods, heated by an induction coil, and cooled using nitrogen gas. A thermocouple was spot-welded in the middle of the specimens to control the temperature.

Different heat treatments were applied above and below the M_s-temperature, after a full austenitization at 900 °C for 240 s. The applied heat treatments are described as follows (Fig. 1):

  (i) A direct-quench treatment was performed to determine the experimental M_s-temperature and the kinetics of the martensite formation. The analysis of the dilatometric curve, presented elsewhere [11], determined an experimental $M_{s\ (1\%)} = 320\ °C\ \pm\ 5\ °C$, at which temperature the volume fraction of martensite formed is 1%.
 (ii) An isothermal treatment above the M_s-temperature was carried out at 340 °C to obtain a microstructure formed by a mixture of bainite, retained austenite and fresh martensite.
(iii) Three isothermal treatments between M_s and room temperature (RT) were performed at 320 °C, 300 °C and 270 °C to obtain a
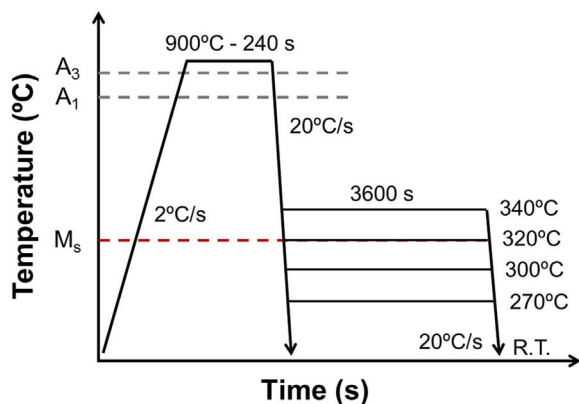

Fig. 1. Schematic representation of the heat treatments applied in the dilatometer to the selected steel.

multiphase microstructure formed by martensite obtained during cooling from austenitization to the isothermal temperature, bainitic ferrite, retained austenite, and fresh martensite obtained in the final cooling to room temperature.

The volume fractions of retained austenite at room temperature were determined by X-ray diffraction (XRD) experiments using a Bruker D8-Advance diffractometer equipped with a Bruker Vantec Position Sensitive Detector. CoKα radiation was used in the 2θ scan from 40° to 130° with a step size of 0.035°. The fractions of austenite and ferrite were calculated by the integrated area method using the (111), (200), (220), and (311) austenite peaks, and the (110), (200), (211), and (220) ferrite peaks [21]. The heat-treated specimens were metallographically prepared by grinding and polishing. 2% Nital etching was applied to the specimens to reveal the microstructure. A pre-analysis of microstructures by Light Optical Microscopy (LOM) and Scanning Electron Microscopy (SEM) was done and presented elsewhere [11].

Electron Back Scatter Diffraction (EBSD) in combination with SEM was used to perform a detailed characterization of the transformation products obtained in the heat treatments previously described. In order to analyse the same area by EBSD and SEM, various micro-indentations (HV1) were made in the specimens to select representative areas. As a final preparation step, the specimens were mechanically polished with a colloidal silica solution in order to exhaustively clean the specimens and remove surface deformation. Areas selected in the specimens were first analysed by EBSD.

The EBSD patterns were acquired on a FEI Quanta 450 scanning electron microscope equipped with a Field Emission Gun (FEG-SEM) by means of the OIM Data Collection software. The analysis was performed under the following conditions: acceleration voltage of 20 kV, spot size 5, working distance of 16 mm, tilt angle of 70°, and step size of 50 nm in a hexagonal scan grid. The orientation data were post-processed with TSL OIM® Analyses 6.0 software. First, a grain confidence index (CI) standarization was applied to the raw data, selecting a tolerance angle of 5° and a minimum grain size of 6 pixels, and considering that grains are formed by multiple pixel rows. The second step of the post-processing procedure included neighbour-orientation correlation with a tolerance angle of 5° and a minimum confidence index of 0.1. Finally, a down-filtering criterion of confidence index higher than 0.1 was applied to reduce the number of pixels poorly indexed, i.e., not attributed to either fcc or bcc phases.

After a comprehensive EBSD analysis, specimens were carefully polished with a colloidal silica solution for 5 to 10 min in order to remove the carbon deposition layer of the specimen surface. Afterwards, 2% Nital etching was applied to the specimens to reveal the different phases formed during the heat treatments. The EBSD-analysed areas were then studied with a JEOL JSM-6500F Scanning Electron Microscope (SEM) using a 15 kV electron beam and the Secondary Electron Imaging (SEI) detection mode.

3. Results and discussion

3.1. Volume fraction of phases

There was no evidence of the formation of ferrite, pearlite, or bainite during the initial cooling to the isothermal temperatures above and below M_s [11]. Only when the temperature decreased below the M_s temperature, a dilatation was observed due to the formation of a certain fraction of athermal martensite prior to the isothermal holding. Afterwards, dilatometric curves showed a significant dilatation during the isothermal holding, which implies the formation of an isothermal product phase identified as bainitic ferrite in ref. [11]. There was also a small deviation from linearity of the dilatometric curves during the final cooling to room temperature, showing the formation of fresh martensite during that cooling. The determination of the volume fractions of product phases obtained in the applied heat treatments is

Table 1
Phase fractions obtained after the application of the selected heat treatments. f^{PM}, f^{BF}, f^{FM}, and f^{RA} are the experimental fractions of Prior Athermal Martensite, Bainitic Ferrite, Fresh Martensite, and Retained Austenite, respectively [11].

Temperature (°C)	f^{PM}	f^{BF}	f^{FM}	f^{RA}
340	–	0.74	0.16	0.10
320	< 0.02	0.84	0.07	0.08
300	0.16	0.71	0.05	0.09
270	0.77	0.12	0.02	0.09

explained in ref. [11] and shown in Table 1.

3.2. Microstructural features

Microstructures were characterized by a combined analysis of SEM and EBSD images in order to find patterns regarding the structure and morphology of the different product phases. Distinct microstructural features with specific characteristics were observed and described in detail below. The descriptions will allow a better characterization and understanding of the nature of the product phases obtained in each isothermal treatment. A schematic representation of these features is shown in Fig. 2. Examples of these microstructural features will be shown in further sections.

3.2.1. Thin features (S_T)

This microstructural feature, defined as 'S_{Thin}' (S_T), appears in the

Structural Feature	Schematic Representation
S_{Thin} (S_T)	Acicular units
$S_{Irregular}$ (S_I)	Irregular shape
S_{Thick} (S_{TK})	Carbides — Sharp tip
$S_{Elongated}$ (S_E)	Wavy Boundary — Carbides
S_{Blocky} (S_B) (MA island)	Small laths — RA

Fig. 2. Schematic representations of the different features described, directly derived from actual micrographs.

form of a thin unit with acicular shape. S_T units are aligned parallel with each other and appear as low-relief microstructures after etching. Their aspect ratio (a/c), where 'a' and 'c' are the length and width, respectively, can vary in a wide range between 5 and 15. The width of S_T units is generally less than 1 μm, and the length varies from 3.5 μm to 15 μm. Most of them have a mean length between 5 and 8 μm and a mean width between 0.6 and 0.8 μm. Carbides are not observed within this type of microstructural feature.

3.2.2. Irregular features (S_I)

This second microstructural feature has an irregular lath-shaped morphology without carbides and is defined as '$S_{Irregular}$' (S_I). These lath-shaped features also appear as low-relief microstructures after etching. The length of the S_I features varies between 4 and 7 μm and the width between 1 and 3 μm, so S_I features are wider than S_T, with a lower aspect ratio.

3.2.3. Thick features (S_{TK})

The third type of microstructural feature appears in the form of laths with a sharp tip at one of its edges. These lath-shaped features are defined as 'S_{Thick}' (S_{TK}). They are aligned parallel and appear as low-relief microstructures after etching. Carbides are generally visible within these features. The aspect ratio of S_{TK} varies in the range of 2.5 to 6. These lath-shaped structures have a mean length and width of 5 μm and 1.1 μm, respectively. S_{TK} features seem to grow from the prior austenite grain boundaries, and are surrounded by S_T units.

3.2.4. Elongated features (S_E)

This fourth microstructural feature presents a big elongated, lath-shaped morphology, so it is defined as '$S_{Elongated}$' (S_E). This type of lath-shaped features are aligned parallel to adjacent constituent units and appear as low-relief microstructures. Their size is larger than that of the previous microstructural features described. S_E features have a mean length and width of 12 μm and 2 μm, respectively. In general, S_E features are longer and wider than S_T. There is an abundant presence of carbides within most of S_E features.

The most relevant characteristic of S_E is the presence of wavy boundaries. These wavy boundaries were first reported by Kim et al. [16], who concluded that the nature of these isothermal products formed below M_s was neither purely martensitic nor purely bainitic. More recently, Somani et al. [17] identified an isothermal product in the form of laths with wavy boundaries, formed during isothermal treatments below M_s. Ledge-like protrusions are also observed in these laths. Somani et al. identified this product phase as isothermal martensite.

3.2.5. Blocky features (S_B) (also known as MA islands)

This microstructural feature is characterized by a blocky structure which combines small parallel aligned laths within the structure with irregular blocks at its boundaries. This feature, defined as 'S_{Blocky}' (S_B), is generally known as martensite-austenite island (MA), which is formed from partly untransformed austenite in the final cooling to room temperature. SEM shows the MA island as a non-etched structure with a smooth surface. However, EBSD analysis displays that the MA island is formed by an internal structure of very small martensite laths surrounded by small blocks of retained austenite (RA) at the boundaries. These small laths appear aligned parallel within the island. The length of the laths is less than 2 μm.

3.3. Microstructures obtained from heat treatments

3.3.1. At 340 °C (above M_s)

According to dilatometry results, bainitic ferrite and fresh martensite coexist in this microstructure in percentages of 74% and 16% volume fractions, respectively (see Table 1), completed by 10% of retained austenite. In this case, there is no formation of athermal
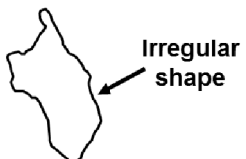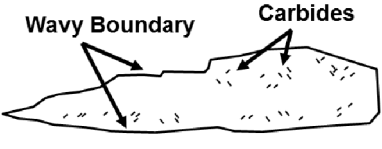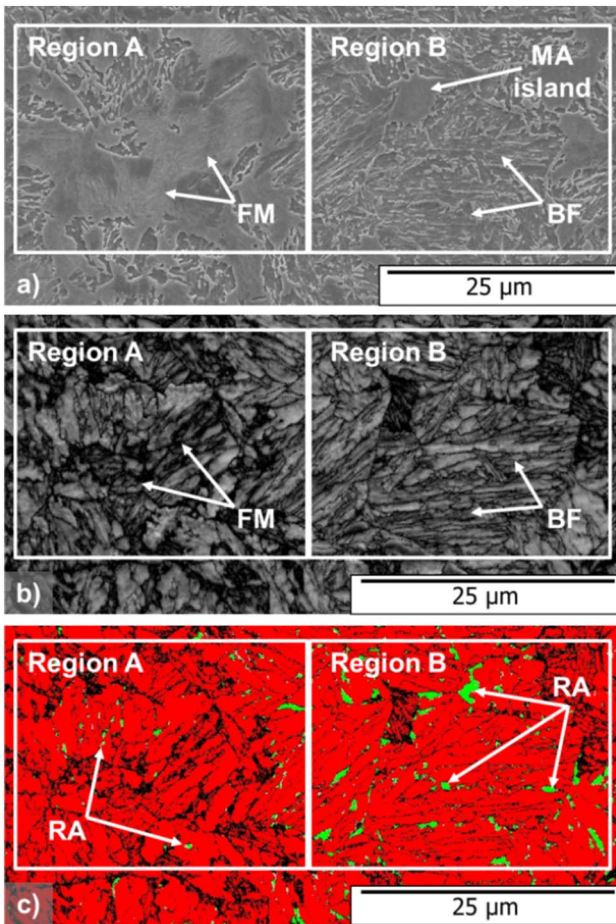
Fig. 3. a) SEM micrograph, b) Image Quality (IQ) map, and c) Phase Distribution (PD) map of a determined area of the specimen isothermally treated at 340 °C (above M_s).

martensite prior to the isothermal treatment. The microstructure is thus a mixture of bainitic ferrite, retained austenite and MA islands. Fig. 3 shows the SEM micrograph, the Image Quality (IQ) map, and the Phase Distribution (PD) map of the same area of the specimen. The combined analysis of images allows to distinguish two different sub-areas: Region A, in which different features of fresh martensite appear in combination with small bainitic ones, and Region B, in which bainitic ferrite is the dominant product phase. Bainitic ferrite mainly appears as S_T features with retained austenite (RA) between them. These bainitic areas are generally better indexed in EBSD than the martensitic ones, so they appear as bright areas in the IQ map due to a higher confidence index (see Fig. 3.b). Conversely, fresh martensite areas have a poorer indexing than the bainitic ones due to internal strains and dislocations. This means that the confidence index will be lower in those areas, and darker regions will appear in the IQ map, as shown in Fig. 3.b.

The distribution and morphology of the retained austenite is also an important factor to distinguish between different product phases. Fig. 3.c shows the Phase Distribution (PD) map of the above-mentioned specimen. As observed, retained austenite (in green) mainly appears within the bainitic ferrite areas (Region B) in the form of small blocks or thin films between bainitic ferrite units. This means that, after the incomplete isothermal transformation (approx. 74% of bainitic ferrite), the remaining austenite in the bainitic areas is more stable than in the areas that become martensitic due to a higher carbon enrichment during the isothermal holding. In the final cooling, while the remaining austenite in bainitic areas will be retained, most of the remaining austenite present in martensitic areas will transform into fresh martensite due to its lower stability. This explains the lower fraction of retained austenite obtained in martensitic areas.

For a detailed description of the different product phases, a prior austenite grain was selected and analysed by a combined study of its SEM micrograph and three different EBSD maps, as shown in Fig. 4. Inverse Pole Figures (IPF) and Kernel Average Misorientation (KAM) maps were used to determine the morphology (size and shape) of the different product phases and the distribution of local grain misorientations, respectively. KAM maps were calculated by considering the 1st
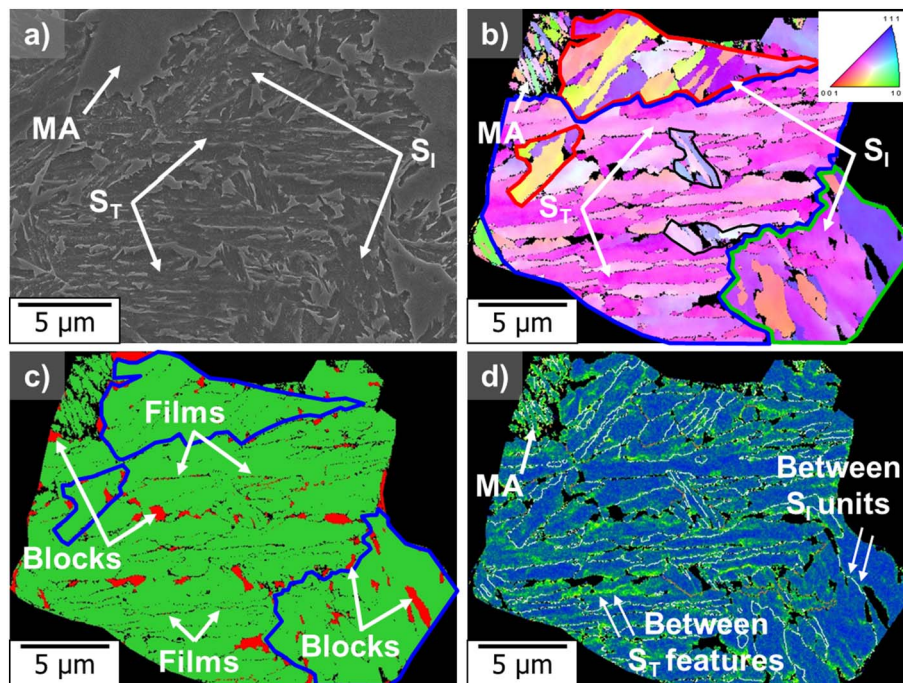

Fig. 4. a) SEM micrograph, b) IPF map, c) PD map, and d) KAM map of a selected prior austenite grain of the specimen isothermally treated at 340 °C. Regions are marked on the IPF map by different colours.

neighbours as the nearest neighbour points of the kernel in order to include information about the surroundings of the measured point.

The selected grain is mainly formed by four regions with different orientation relationships (ORs) (see Fig. 4.b). Analysing the central region of the austenite grain (marked by a blue contour), a typical bainitic structure can be distinguished, which is mainly formed by S_T features. Retained austenite appears in the form of very thin films between the units (see Fig. 4.c). Elongated blocky structures of retained austenite are also distinguished close to region boundaries and at the boundaries of the MA island, as shown in Fig. 4.c.

S_I features can be observed in the microstructure (see Fig. 4.a, b). Although the morphology of these laths is not acicular, their nature may be bainitic. The reason for this proposition is that there is no dilatometric evidence of the formation of prior athermal martensite, so bainitic ferrite cannot be confused with tempered martensitic structures in this microstructure. Fig. 4 also shows a martensite-austenite (MA) island in which its internal structure of small martensite laths can be observed (Fig. 4.b). The KAM map (Fig. 4.d) shows that these martensitic structures present higher concentrations of local misorientation than the bainitic ones, so the internal structure is more distorted. The KAM map also shows that higher local misorientations are concentrated at the boundaries between S_T features, and/or between S_I units, as shown in Fig. 4.d (white arrows).

3.3.2. At 320 °C (at M_s)

This isothermal temperature corresponds to the experimental M_s-temperature at 1%, i.e., when the volume fraction of martensite formed is approximately 1%. This prior athermal martensite formed during cooling from austenitization to the isothermal temperature will be tempered during the isothermal holding, so its appearance will be different from that of the fresh martensite obtained in the final cooling. A complex multiphase microstructure is thus obtained at this temperature (see Table 1), where bainitic ferrite represents more than 80% of the volume fraction.

S_T features containing films of retained austenite appear in the microstructure, as shown in Fig 5.a. and 5.b. According to the previous characterization done above M_s, these features correspond to bainitic ferrite structures. MA islands can also be distinguished in the microstructure (see Fig. 5.a). S_{TK} features are also present at this temperature with their characteristic sharp tip at one of the edges. These lath-shaped structures are different from the ones identified at 340 °C, above M_s. Fig. 6.a shows an S_E feature, i.e., a large elongated lath containing carbides. This S_E feature presents wavy boundaries, which can be observed in Fig. 6.b (marked with white arrows) and 6.c (marked with blue dashed line). In addition to this specific characteristic, ledge-like protrusions can be observed in one of the boundaries of this S_E feature (see Fig. 6.b, c). Since these two types of features are not present in microstructures above M_s, they should correspond to martensitic structures, which are tempered during the isothermal holding of the heat treatment.
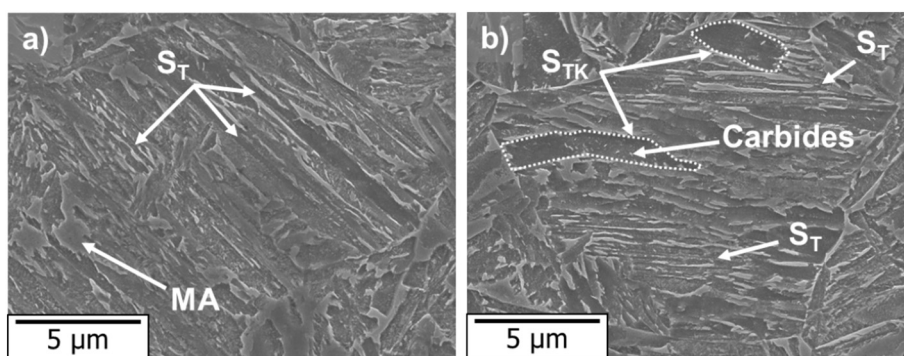
Retained austenite is present in this microstructure in two different morphologies. Within S_T features, retained austenite generally appears as thin films. In S_E features, however, retained austenite appears in the form of elongated blocks along boundaries and/or as irregular blocks between ledge-like protrusions, as shown in Fig. 6.c. The KAM map shows high local misorientations at the boundaries of the S_E feature, as shown in Fig. 6.d (white arrows). Lower local misorientations are also observed within the S_E feature, which can correspond to low-angle boundaries of its internal structure.

3.3.3. At 300 °C (below M_s)

At this temperature, a volume fraction of approximately 16% of prior athermal martensite is formed during the cooling below M_s until reaching the isothermal temperature. This prior athermal martensite will be tempered during the isothermal holding. The microstructure is thus a mixture of bainitic ferrite, prior athermal martensite, and MA islands (see Table 1). S_T features, identified as bainitic ferrite in previously described microstructures, are shown in Fig. 7. This indicates the formation of bainitic ferrite in isothermal treatments below M_s with similar morphological characteristics as the bainite formed in treatments above and at the M_s temperature.

Other types of product phases can be distinguished in this microstructure. Fig. 8 shows the SEM micrograph, Inverse Pole Figure (IPF), Phase Distribution (PD), and Kernel Average Misorientation (KAM) maps of a specific prior austenite grain of the specimen treated at 300 °C. An S_E feature with wavy boundaries can be observed at the top part of the grain (marked with a dashed blue line). This specific feature has also been observed in microstructures formed during isothermal treatments at 320 °C (at M_s). As pointed out in the microstructural description of that heat treatment, S_E features should be characterized as martensite since this type of feature does not appear in treatments above M_s and its presence in the microstructures becomes more pronounced when the volume fraction of prior athermal martensite increases. Carbides are visible within these S_E features, and there seem to be multi-directional carbides. Bainitic structures are also characterized at this temperature in the form of S_T and S_I features (see Fig. 8.a, b).

Fig. 8.a also shows an interesting feature in the surroundings of S_E. This feature corresponds to very small acicular units (S_T features), identified as bainitic ferrite, just next to the wavy boundary of the lath. These S_T features are indicated by a dashed white or red oval in the SEM figure and EBSD maps. As observed in Fig. 8.a, the S_T features seem to grow from the S_E and appear aligned at both sides of the lath-shaped S_E. However, in the EBSD maps (Fig. 8.b, c, d), there is no clear indication of the existence of these features, apart from a small concentration of high local misorientations (see Fig. 8.d). According to the analysis, bainitic ferrite (S_T) may be growing from the prior athermal martensite (S_E), maintaining a similar crystallographic orientation relationship. This fact could contribute to the formation of the ledge-like protrusions which can give rise to a wavy appearance of the boundaries of the lath-
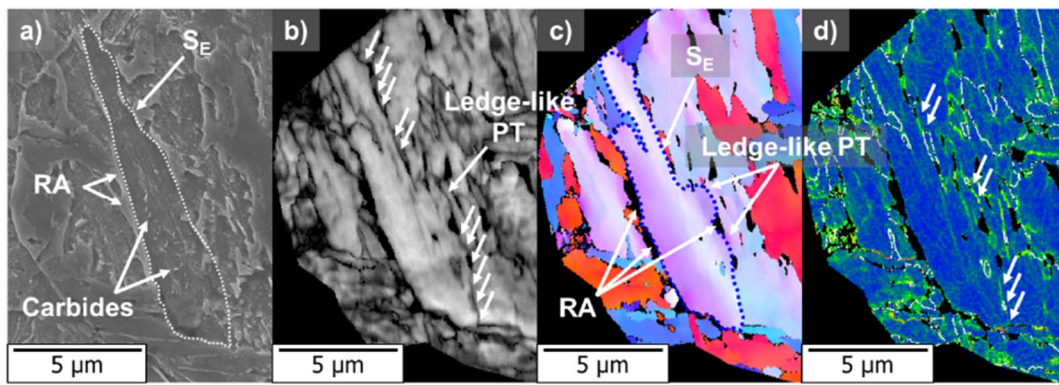

Fig. 5. SEM micrographs of two determined areas of the specimen isothermally treated at 320 °C (at M_s), showing the presence of S_{Thin} and S_{Thick} features in a selected prior austenite grain.

Fig. 6. a) SEM micrograph, b) IQ map, c) IPF map, and d) KAM map of a region within a prior austenite grain of the specimen isothermally treated at 320 °C.
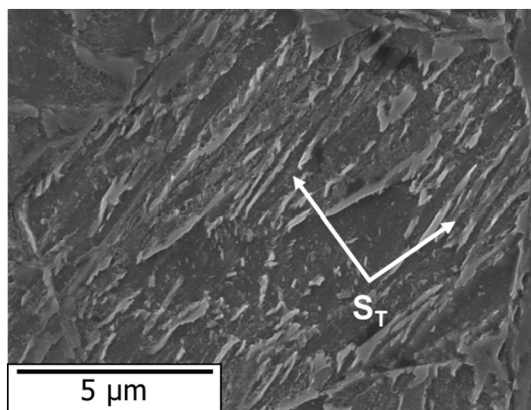

Fig. 7. Presence of S_{Thin} microstructural features in the specimen isothermally treated at 300 °C (below M_s).

shaped S_E features.

Retained austenite mainly appears in the form of small elongated blocks, as shown in Fig. 8.c. These blocks could form a continuous film at the boundaries between microstructural constituents, as marked by the dashed white line in Fig. 8.c. A high density of low-angle boundaries with misorientations lower than 5–7° can be observed in Fig. 8.d (marked with white arrows). These boundaries separate the different sub-units present within the same microstructural constituent. The described boundaries coincide with the discontinuous "films" of retained austenite.

3.3.4. At 270 °C (below M_s)

At 270 °C, 50 °C below the experimental M_s-temperature, almost 80% of the microstructure is formed by prior athermal martensite, which is tempered, with only 12% of bainitic ferrite formed during the isothermal holding (see Table 1) and 9% of retained austenite. The microstructure is mainly formed by lath-shaped structures of different sizes and shapes, containing carbides inside (see Fig. 9.a). In this case, no bainitic structures similar to the ones described to be formed above M_s are observed. Although the studied steel has a 1.5 wt. percent silicon content, carbide precipitation is not completely supressed.

Fig. 9.a shows two types of microstructural features: S_{TK} and S_E. Wavy boundaries with ledge-like protrusions, a specific microstructural characteristic of S_E, can be observed in Fig. 9.b, c. Retained austenite is also present in this microstructure in the form of elongated blocks between S_E features (see Fig. 9.c). Fig. 10 shows another example of S_E features, which are characteristic for this microstructure. The S_E feature, indicated by a dashed white contour in Fig. 10.a, is extended along the grain from one boundary to the opposite one. This specific lath-shaped structure is characterized by wavy boundaries at its both sides, marked with dashed blue lines in Fig. 10.b. The KAM map shows high local misorientations at the wavy boundaries of the S_E feature (see Fig. 10.c).

According to volume fractions obtained and previous microstructural analysis at higher temperatures, both features S_{TK} and S_E are definitively characterized as prior athermal martensite, tempered during the isothermal holding. As described in the microstructural characterization at 300 °C, the existence of ledge-like protrusions may produce the characteristic wavy boundaries observed in S_E. Although there are carbides along the entire S_E feature, these protrusions do not present any carbides inside, as shown in Fig. 9.a. Based on the EBSD maps (Fig. 9.b, c), the protrusions exhibit a similar orientation as the rest of the S_E feature. As is pointed out for the microstructure formed at 300 °C, these protrusions can correspond to bainitic ferrite structures growing from the prior athermal martensite.
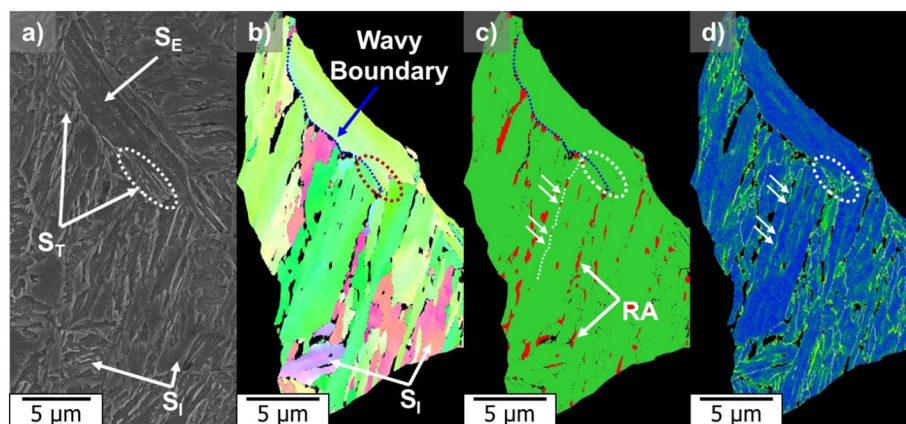

Fig. 8. a) SEM micrograph, b) IPF map, c) PD map, and d) KAM map of a selected prior austenite grain of the specimen isothermally treated at 300 °C.
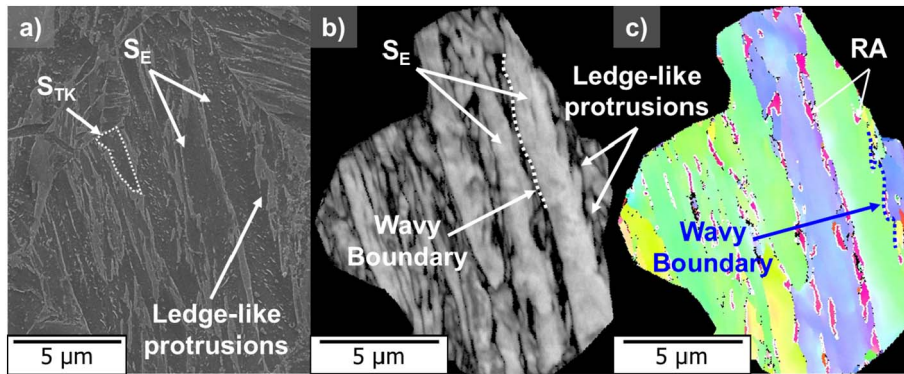
Fig. 9. a) SEM micrograph, b) IQ map, and c) IPF map of a selected prior austenite grain of the specimen isothermally treated at 270 °C. This specimen contains a volume fraction of prior athermal martensite of approximately 80%. This martensite is tempered during the isothermal holding.

3.4. Nature of product phases

Table 2 shows a summary of the main characteristics of the five microstructural features observed in the analysis of the four isothermal treatments performed at 340 °C (above M_s), and 320 °C (at M_s), 300 °C, and 270 °C (below M_s), as well as at which temperature that specific feature was observed. The possible nature of the each microstructural feature is also specified.

Considering the thermal cycle followed in these heat treatments, the bainitic structures, S_T and S_I, were only formed during the isothermal holdings of one hour performed at temperatures of 300 °C and higher. However, the martensitic structures, S_{TK} and S_E, were previously formed during the cooling from austenitization to the selected isothermal temperature. MA islands were finally formed in the cooling to room temperature from the remaining austenite, which was not fully transformed during the isothermal holding.

As shown in Table 2, S_T and S_I are considered bainitic structures since they are the main features observed in the isothermal treatment performed above M_s, where there is no formation of athermal martensite prior to the isothermal holding. Both types of features are also observed in isothermal treatments below M_s. Besides, S_{TK} and S_E are considered martensitic structures. The reason for this conclusion is the majority presence of these two microstructural features after applying the isothermal treatment at 270 °C (below M_s), where almost 80% of the volume corresponds to the prior athermal martensite formed during cooling until reaching the isothermal temperature. Furthermore, as the isothermal temperature below M_s is increased and approaches M_s, the presence of these microstructural features in the microstructures is reduced. Martensite-austenite islands, formed in the final cooling to room temperature, are present in the microstructures of all heat treatments.

The martensitic nature of S_E is partially in agreement with previous investigations done by Kim et al. [16] and Somani et al. [17]. Both

authors characterized an isothermal product with wavy boundaries and ledge-like protrusions in isothermal treatments performed below M_s in low-carbon steels with similar compositions as the one investigated in the present work. In both studies, the authors conclude that the nature of these laths with wavy boundaries is not purely bainitic since they have a stronger similarity with athermal martensite. However, there are some descriptive details which differ between each characterization. These characterization details are presented as follows:

1. Kim et al. [16] compare by TEM observations the product phases obtained in an isothermal treatment above M_s, below M_s (with 10% of prior athermal martensite), and in a direct quench. The authors suggest that the presence of wavy boundaries containing ledges in the mentioned laths formed below M_s is the result of the thickening of those laths during the isothermal transformation. Additionally, multi-variant carbides were also distinguished within those isothermal laths and the athermal martensite, but not in lower bainite. Kim et al. thus state that although there was a stronger similarity with athermal martensite than with lower bainite, the nature of those isothermal laths is neither purely martensitic nor purely bainitic.

2. Somani et al. [17] also compared by TEM observations the nature of the different products phases obtained during two-step quenching and partitioning (Q & P) treatments. Such isothermal laths with wavy boundaries and ledge-like protrusions were also characterized. In this case, these laths are considered the result of the isothermal growth, through the migration of ledges, during the partitioning step of the prior athermal martensite laths already formed. These laths were thus identified as martensite.

Although both identifications are feasible, the thermal conditions of the heat treatments analysed in each investigation are different between them and with respect to the present work. In the investigation
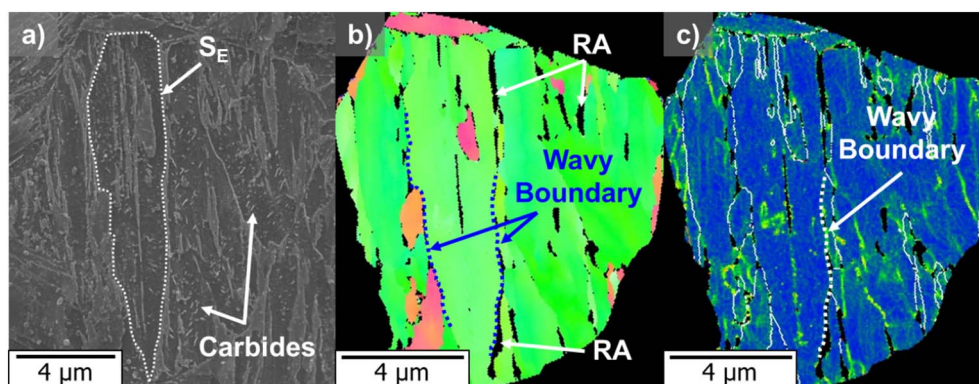

Fig. 10. a) SEM micrograph, b) IPF map, and c) KAM map of a selected prior austenite grain of the specimen isothermally treated at 270 °C.

Table 2

Summary of the microstructural features observed in isothermal treatments at 340, 320, 300, and 270 °C. The nature and characteristics of each feature are also detailed.

Structural feature	Characteristics	340 °C	320 °C	300 °C	270 °C	Phase nature
S_{Thin} (S_T)	- Above and below M_s. - Thin units with acicular shape. - Parallel aligned. - Length: 5–8 μm. - No carbides distinguished.	✓	✓	✓	?	*Bainitic*
$S_{Irregular}$ (S_I)	- Above and below M_s. - Laths with irregular shape. - Wider than S_T. - No carbides distinguished.	✓	✓	✓	–	*Bainitic*
S_{Thick} (S_{TK})	- Below M_s. - Laths with sharp tip at an edge. - Surrounded by S_T. - Contain carbides.	–	✓	✓	✓	*Martensitic*
$S_{Elongated}$ (S_E)	- Below M_s. - Longer and wider than S_T. - Wavy boundaries. - Contain carbides.	–	✓	✓	✓	*Martensitic*
S_{Blocky} (S_B) (*MA island*)	- Smooth surface (not etched). - Internal structure. - Very small laths. - Surrounded by RA blocks.	✓	✓	✓	✓	*Martensite/austenite*

of Kim et al., there is no microstructural characterization of existing tempered martensite formed in the treatment below M_s (with 10% volume fraction), so those S_E features could also be considered as tempered martensite. In the investigation of Somani et al., the nature of S_E is certainly considered martensitic.

However, there is another possible explanation which has not been considered yet. The formation of bainitic ferrite below M_s could be the reason of the appearance of ledge-like protrusions in the S_E features, which lead to the formation of wavy boundaries. Several studies have shown that the formation of athermal martensite prior to isothermal treatments leads to the creation of new potential nucleation sites in the form of martensite-austenite interfaces [8–11]. At the same time, as the isothermal temperature decreases and approaches M_s, there is a reduction in the size of the bainitic units due to an increase of the transformation kinetics. The lower the temperature, the higher the undercooling and driving force for nucleation. So, very small units of bainitic ferrite may grow from the initial martensitic laths (S_E features) in the form of ledge-like protrusions at the very beginning of the isothermal treatments below M_s.

This fact can be observed in the microstructure obtained after the isothermal treatment at 300 °C (below M_s), shown in Fig. 8.a. In that figure, small units of a few micrometres length (less than 5 μm) appear just next to the wavy boundary of an S_E feature. The morphology (shape and size) of these units strongly differs from the one of the S_E, so they can be considered as different product phases. Their orientation may be the same (or similar) to that of the main S_E feature (see Fig. 8.b). Only a small concentration of local deformation around the area where those small units appear (see Fig. 8.d) indicates their possible existence. Although these observations can suggest the different nature of these ledge-like protrusions in treatments below M_s, further investigations are needed for a detailed characterization of these protrusions and a better understanding of the interactions between prior athermal martensite and the subsequently formed bainitic ferrite.

4. Conclusions

The nature of the different microstructural features obtained in isothermal treatments below M_s is determined as bainitic or martensitic by comparing experimental volume fractions of the product phases,

which were extracted from previous dilatometry and XRD analysis, with the morphology (size and shape) of the specific features characterized at each isothermal temperature by SEM and EBSD analysis. The main conclusions obtained from this methodology are the following:

1. Bainitic ferrite appears in the form of thin acicular units and/or irregularly shaped laths in isothermal treatments performed above and below the M_s-temperature. Acicular units are aligned parallel to each other. They have a mean length between 5 and 8 μm and a mean width between 0.6 and 0.8 μm. Irregular laths are wider than acicular units. Carbides are not observed within any of these features.
2. Martensite appears as lath-shaped structures in isothermal treatments performed below the M_s-temperature. Two different martensitic structures are characterized in the form of laths with a characteristic sharp tip at one of the edges and/or laths presenting wavy boundaries with ledge-like protrusions. The latter martensitic structures are longer and wider than acicular units of bainitic ferrite, with a mean length and width of 12 μm and 2 μm, respectively. Both types of lath-shaped structures contain carbides within them. Based on the characterization methodology described above, these microstructures correspond well to tempered martensite.
3. Martensite-austenite islands are characterized in all isothermal treatments performed above and below M_s. These islands present an internal structure formed by very small martensite laths (smaller than 2 μm) parallel aligned, surrounded by retained austenite blocks.
4. The appearance of some protrusions in martensitic structures can be related to the formation of bainitic ferrite in isothermal treatments below M_s, which might lead to the formation of wavy boundaries in such martensitic laths.

through the VIDI-Grant 12376.

References

[1] K. Sugimoto, T. Ilda, J. Sakaguchi, T. Kashima, Retained austenite characteristics and tensile properties in a TRIP type bainitic sheet steel, ISIJ Int. 40 (2000) 902–908.

[2] K. Sugimoto, M. Murata, S.M. Song, Formability of Al-Nb bearing ultra-high strength TRIP-aided sheet steels with bainitic ferrite and/or martensite matrix, ISIJ Int. 50 (2010) 162–168.

[3] Y. Jiang, R. Zhou, R. Zhou, D. Lu, Z. Li, Microstructures and properties of a bainite and martensite dual-phase cast steel fabricated by combination of alloying and controlled cooling heat treatment. Trans. Tech. Publications, Mater. Sci. Forum 475–479 (2005) 93–96.

[4] S.M.C. Van Bohemen, M.J. Santofimia, J. Sietsma, Experimental evidence for bainite formation below M_s in Fe-0.66C, Scr. Mater. 58 (2008) 488–491.

[5] J.C. Hell, M. Dehmas, S. Allain, J.M. Prado, A. Hazotte, J.P. Chateau, Microstructure-properties relationships in carbide-free bainitic steels, ISIJ Int. 51 (2011) 1724–1732.

[6] I.A. Yakubtsov, G.R. Purdy, Analyses of transformation kinetics of carbide-free bainite above and below the athermal martensite start temperature, Metall. Mater. Trans. A 43A (2012) 437–446.

[7] D. Kim, J.G. Speer, B.C. De Cooman, The isothermal transformation of low-alloy low-carbon CMnSi steels below M_s. Trans. Tech. Publications, Mater. Sci. Forum 654–656 (2010) 98–101.

[8] H. Kawata, K. Hayashi, N. Sugiura, N. Yoshinaga, M. Takahashi, Effect of martensite in initial structure on bainite transformation, Mater Sci Forum 638-642 (2010) 3307–3312.

[9] M.J. Santofimia, S.M.C. van Bohemen, D.N. Hanlon, L. Zhao, J. Sietsma, Perspectives in high-strength steels: Interactions between non-equilibrium phases, Inter. Symp. on AHSS, AIST, 2013, pp. 331–339.

[10] L. Zhao, L. Qian, J. Meng, Q. Zhou, F. Zhang, Below-M_s austempering to obtain refined bainitic structure and enhanced mechanical properties in low-C high-Si/Al steels, Scr. Mater. 112 (2016) 96–100.

[11] A. Navarro-López, J. Sietsma, M.J. Santofimia, Effect of prior athermal martensite on the isothermal transformation kinetics below M_s in a low-C high-Si steel, Metall. Mater. Trans. A 47A (2016) 1028–1039.

[12] P. Kolmskog, A. Borgenstam, M. Hillert, P. Hedstrom, S.S. Babu, H. Terasaki, Y.I. Komizo, Direct observation that bainite can grow below M_s, Metall Mater Trans A 43A (2012) 4984–4988.

[13] E.P. Da Silva, D. De Knijf, W. Xu, C. Föjer, Y. Houbaert, J. Sietsma, R. Petrov, Isothermal transformations in advanced high strength steels below martensite start temperature, Mater Sci Technol 31 (2015) 808–816.

[14] S. Samanta, P. Biswas, S. Giri, S.B. Singh, S. Kundu, Formation of bainite below the M_s temperature: kinetics and crystallography, Acta Mater 105 (2016) 390–403.

[15] D. Kim, J.G. Speer, B.C. De Cooman, Isothermal transformation of a CMnSi steel below the M_s temperature, Metall. Mater. Trans. A 42A (2011) 1575–1585.

[16] D. Kim, S.J. Lee, B.C. De Cooman, Microstructure of low carbon steel isothermally transformed in the M_s to M_f temperature range, Metall. Mater. Trans. A 43A (2012) 4967–4983.

[17] M.C. Somani, D.A. Porter, L.P. Karjalainen, R.D.K. Misra, On various aspects of decomposition of austenite in a high-Si steel during Q&P, Metall. Mater. Trans. A 45A (2014) 1247–1257.

[18] S.R. Pati, M. Cohen, Nucleation of the isothermal martensitic transformation, Acta Metall 17 (1969) 189–199.

[19] A. Borgenstam, M. Hillert, J. Agren, Critical temperature for growth of martensite, Acta Metall Mater 43 (1995) 945–954.

[20] A. Borgenstam, M. Hillert, Activation energy for isothermal martensite in ferrous alloys, Acta Mater 45 (1997) 651–662.

[21] C.F. Jatczak, J.A. Larson, S.W. Shin, Retained austenite and its measurements by X-ray diffraction, 453 Society of Automotive Engineers, 1980Special Publication.